# A Low Mechanical Noise Tri-axis MEMS Inertial Sensor Fabricated by Multi-Layered Metal Technology

Daisuke Yamane[1,2*], Toshifumi Konishi[3], Hiroshi Toshiyoshi[1,2], Kazuya Masu[1,2] and Katsuyuki Machida[1,2,3]

[1]CREST, Japan Science and Technology Agency, Kawaguchi, 332-0012, Japan
[2]Tokyo Institute of Technology, Yokohama, 226-8503, Japan
[3]NTT Advanced Technology Corporation, Atsugi, 243-0124, Japan
[4]The University of Tokyo, Tokyo, 153-8904, Japan
[*]E-mail: yamane.d.aa@m.titech.ac.jp

Keywords: Mechanical noise, Tri-axis, MEMS, Inertial sensor, Multi-layered metal, Electroplating

Abstract

MEMS accelerometers are used in various consumer electronics. Further performance advancement is required for the accelerometers to achieve wide sensing range and high resolution for promising application such as inertial measurement units [1]. For multi-axis acceleration sensing, tri-axis single proof mass MEMS accelerometer could substantially reduce the device footprint when compared with single-axis single proof mass device. For this background, we have proposed single- [2] and dual- [3] axis MEMS capacitive inertial sensors by using multi-layered metal technology that employ high-density material to shrink the size of proof mass. The high-density material has enabled to reduce the Brownian noise equivalent acceleration ($B_N$) [4], which is inversely proportional to the proof mass. In this paper, we present the mechanical noise evaluation of a tri-axis single proof mass MEMS inertial sensor fabricated by multi-layered metal technology. The fabrication process and the design concept of the tri-axis sensor is shown in Fig. 1. The fabrication process is based on gold electroplating and compatible with post-CMOS (complementary metal-oxide semiconductor) process [5]. Since the $B_N$ is inversely proportional to the proof mass, high-density proof mass made of gold ($19.3 \times 10^3$ kg/m$^3$, at 293 K) can achieve lower $B_N$ than that of conventional MEMS accelerometers made of silicon ($2.33 \times 10^3$ kg/m$^3$, at 293 K), when compared with the same device size. The sensor has a fixed bottom electrode (Fig. 1(d)) for Z-axis sensing and four sets of fixed side electrodes (Fig. 1(e)) for X- and Y-axis sensing. An $SiO_2$ layer is formed on the bottom electrode to avoid stiction with the proof mass. Stopper structures are used to limit proof mass motion to prevent the MEMS structures from self-destruction. Fig. 2 shows the developed tri-axis MEMS inertial sensor. The target acceleration sensing range was set to be ±3 G (1 G = 9.8 m/s$^2$), and the $B_N$ was designed to be below 10 μG/Hz$^{1/2}$ for sub-0.1G sensing [3]. Fig. 3 shows the measured capacitance and phase as a function of frequency. From the measurements, we experimentally obtained the resonant frequency and the quality factor of the developed sensor on each axis. Table I summarizes the measured and design characteristics of the tri-axis MEMS inertial sensor. The quality factors and the $B_N$ were designed by using damping coefficient of $1.85 \times 10^{-5}$ N·s/m, temperature of 300 K, and the Boltzmann constant of $1.85 \times 10^{-23}$ J/K. The actual proof mass was obtained by measuring the surface profile of the device. On each sensing axis, the experimentally evaluated $B_N$ has a good agreement with the design value; the evaluated $B_N$s were more than one order of magnitude lower than those of conventional MEMS accelerometers made of silicon. From the results, we confirmed the low mechanical noise characteristics of the proposed device.

Acknowledgement: This work is supported by JSPS KAKENHI Grant Number 15K17453.

References:

[1] N. Yazdi, F. Ayazi, and K. Najafi, *Proc. IEEE* 86, pp. 1640-1659 (1998).
[2] D. Yamane, T. Konishi, T. Matsushima, K. Machida, H. Toshiyoshi, K. Masu, and K. Machida, *Microsystem Technologies*, (2015) in press.
[3] D. Yamane, T. Konishi, T. Matsushima, K. Machida, H. Toshiyoshi and K. Masu, *Appl. Phys. Lett.*, **104** (2014) 074102..
[4] H. Kulah, J. Chae, N. Yazdi, and K. Najafi, *IEEE J. Solid-State Circuits*, 41, pp. 352-361 (2006).
[5] K. Machida, T. Konishi, D. Yamane, H. Toshiyoshi, K. Masu, *ECS Trans.*, **61** (2014) 21-39.

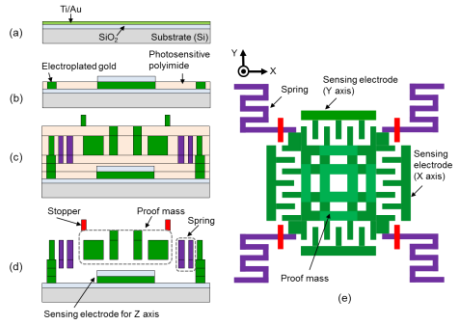


Figure 1. Fabrication process of the tri-axis MEMS inertial sensor. (a) Seed layer deposition, (b) 1st metal, (c) 2nd ~ 6th metal, (d) sacrificial layer release, and (e) top view of the device.

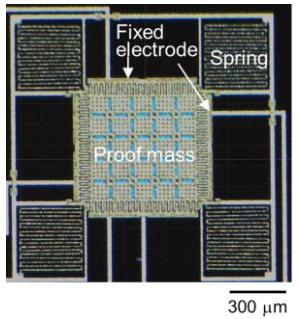


Figure 2. Chip photograph of the developed MEMS sensor.

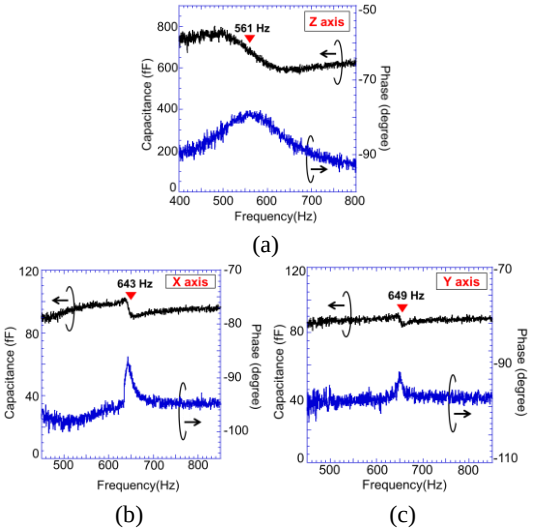


Figure 3. Measured capacitance and phase as a function of frequency. (a) Z-axis, (b) X-axis, and (c) Y-axis

*Design value at room temperature

| | Axis (Sensing range ±3G) | | |
|---|---|---|---|
| | Z | X | Y |
| Proof mass(kg) | $5.80 \times 10^{-8}$ ($5.27 \times 10^{-8}$)* | | |
| $f_{res}$ (Hz) | 561 (872)* | 643 (667)* | 649 (668)* |
| Quality factor | 4.8 (16)* | 15 (12)* | 47 (12)* |
| $B_N$ (μG/√Hz) | 0.37 (1.1)* | 0.26 (1.1)* | 0.21 (1.1)* |

G : 9.8 [m/s$^2$]
$f_{res}$: Mechanical Resonant Frequency
$B_N$: Brownian Noise

Table I. Measured and design characteristics.